Dalton Transactions

Accepted Manuscript

This article can be cited before page numbers have been issued, to do this please use: H. Huang, P. Zhang, Y. Chen, L. Ji and H. Chao, *Dalton Trans.*, 2015, DOI: 10.1039/C5DT02446C.

ROYAL SOCIETY OF CHEMISTRY

www.rsc.org/dalton

View Article Online
DOI: 10.1039/C5DT02446C

The present study demonstrated that the anticancer activities of labile Ru(II) complexes can be efficiently tuned by chelating with different phenyl-substituted terpyridyl ligands.

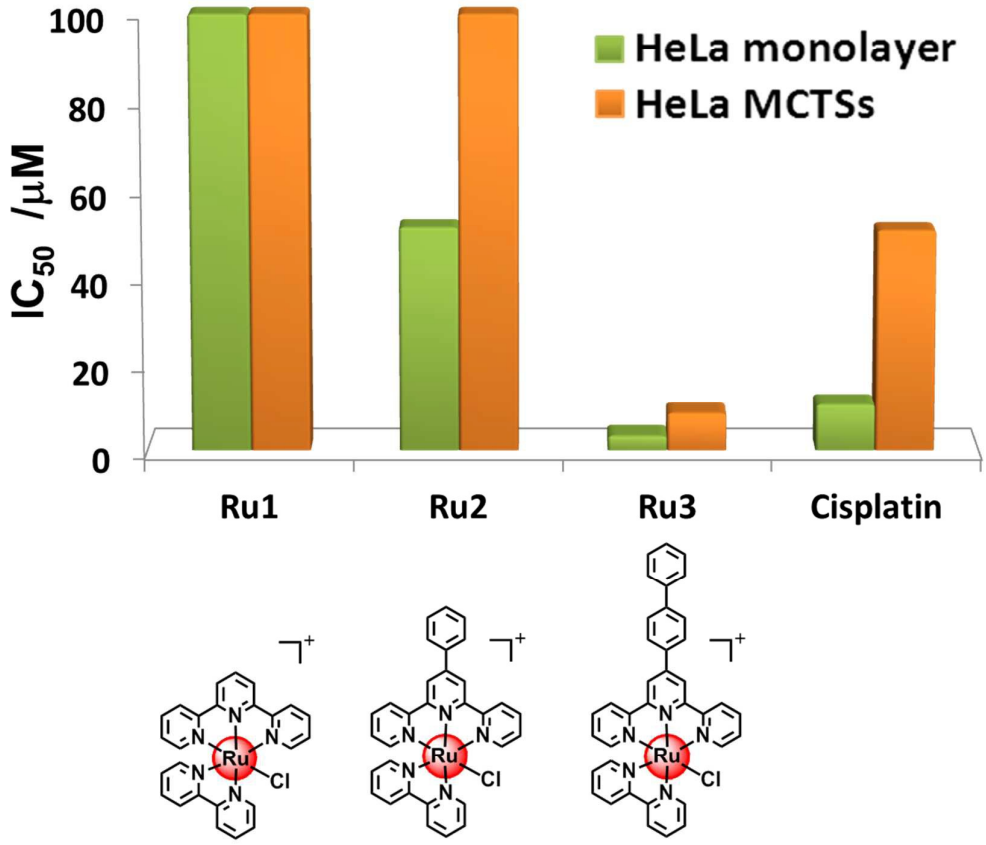

View Article Online
DOI: 10.1039/C5DT02446C

Cite this: DOI: 10.1039/c0xx00000x

www.rsc.org/dalton

PAPER

Labile ruthenium(II) complexes with extended phenyl-substituted terpyridyl ligands: synthesis, aquation and anticancer evaluation†

Huaiyi Huang, Pingyu Zhang, Yu Chen, Liangnian Ji* and Hui Chao*

Received (in XXX, XXX) Xth XXXXXXXXX 20XX, Accepted Xth XXXXXXXXX 20XX
DOI: 10.1039/b000000x

Ruthenium complexes have been considered as promising substitution of cisplatin in cancer chemotherapy. However, the novel ruthenium-based therapies faced with some limitations, such as unimpressive cytotoxicity toward solid tumor. Herein, we designed and synthesized phenyl-substituted terpyridyl ruthenium(II) complexes $[Ru(tpy)(bpy)Cl]^+$ (**Ru1**) $[Ru(phtpy)(bpy)Cl]^+$ (**Ru2**) and $[Ru(biphtpy)(bpy)Cl]^+$ (**Ru3**) which exhibited sharply different anticancer activity. **Ru1-Ru3** all underwent moderate aquation in buffer solution and this process was significantly inhibited by high chloride concentration. **Ru3** was relatively hydrophobic and could be readily uptake by cancer cells as quantified by inductively coupled plasma mass spectrometry (ICP-MS). **Ru1** was non-cytotoxic (IC_{50} >100 μM) while **Ru3** exhibited very promising cytotoxicity on both two-dimensional (2D) cancer cell monolayer and 3D MCTSs. Antiproliferative assay revealed that **Ru3** significantly inhibited cellular DNA replication which induced ultimately apoptosis of cancer cells.

Introduction

DNA transcription and replication accelerates in cancer cells which make cell nucleus an emerging target for chemotherapeutic intervention.[1-4] Cisplatin, the widely used chemotherapy agent, form Pt-DNA crosslink which distorting DNA structure, blocking DNA replication and inducing cancer cells apoptosis.[5] However, severe side effects and drug resistance restrict its clinical application and have fostered interest in exploiting alternative metallodrugs.[6] During the last 20 years, ruthenium (II/III) complexes have emerged in the literature and gradually regarded as promising alternatives to cisplatin.[7] So far, three Ru(III) complex NAMI-A, KP1019 and KP1339 are undergoing clinical trials.[8] Ruthenium complexes have certain advantages over platinum anticancer agents. Ruthenium complexes exhibit lower ligand aquation propensity than platinum complexes. The cationic ruthenium complexes provide better solubility while the octahedral structures result in diverse DNA coordination modes, including covalent binding, groove binding, electrostatic interaction, intercalation and insertion.[9-10] Besides, ruthenium complexes can mimic ferrum binding to transferrin and thus be transported directly to cancer cells, since transferrin receptors were over-expressed at the surface of cancer cells than normal cells.[11] Thus, ruthenium complexes and lower toxicity toward normal tissue than cisplatin. Moreover, ruthenium complexes induce cell death through mechanisms differ from cisplatin which render them active against cisplatin-resistant cell lines.[12-15] However, the novel Ru-based therapies also faced with some limitations, such as poor water stability or unimpressive cytotoxicity toward solid tumor.[16]

Recently, cellular uptake efficiency of metal-complex has gradually gained more and more attention, since the limited penetration of cytotoxic drugs into solid tumors leads to the frequent failure of chemotherapy to completely eradicate tumors in clinic.[17] Traditional 2D cancer cell monolayer is a simplified and widespread cell model for *in vitro* anticancer drug screening. However, cell monolayer inevitably presents limitations in reproducing the complexity and pathophysiology of tumors.[18-21] Cells within solid tumor reflect reduced drug penetration or pathophysiological differences such as hypoxia region and relatively slow cell cycling. As a result, some experimental drugs may be exclusively effective in cancer cell monolayer but non-effective in solid tumors. For example, doxorubicin shows limited penetration into the solid tumors with only 40-100 μm diffusion from blood vessels.[22] Moreover, the discovery of multidrug resistance (MDR) in solid tumor highlighted the differences between cancer cell monolayer and solid tumor.[23] Multicellular tumor spheroids (MCTSs) are 3D heterogeneous cellular aggregates that have been gradually accepted as a valid cell model to mimic the features of *in vivo* solid tumor.[24-25] MCTSs provide insight into metabolic properties similar to solid tumor profiles such as nutrient and oxygen gradients, hypoxic/necrotic regions, cell-cell matrix interactions and gene expression.[26-28] MCTSs thus bridge the gap between the oversimplified cancer cell monolayer and the highly complex nature of solid tumor. MCTSs optimize anticancer drug screening and increase the accuracy to predict *in vivo* anticancer activity before animal studies.

In this paper, we reported three terpyridyl Ru(II) complex with different phenyl-substituted ligand: $[Ru(tpy)(bpy)Cl]^+$ (tpy = 2,2':6',2"-terpyridine, bpy = 2,2'-bipyridine, **Ru1**), $[Ru(phtpy)(bpy)Cl]^+$ (phtpy = 4'-phenyl-2,2':6',2"-terpyri-dine,

View Article Online
DOI: 10.1039/C5DT02446C

Ru2) and $[Ru(biphtpy)(bpy)Cl]^+$ (biphtpy = 4'-biphenyl-2,2':6',2"-terpyridine, **Ru3**) as anticancer agents. The aquation reactivity, DNA binding activity, *log* $P_{o/w}$ values, cellular uptake efficiency and cell cytotoxicity of **Ru1-Ru3** were studied. We found that the length of phenyl-substituent on terpyridyl ligand had a dramatic effect on biological activity of terpyridyl Ru(II) complexes.

Experimental

Materials and Instrument

All solvents were of analytical grade. Ruthenium chloride hydrate, 2,2′-bipyridine (bpy), 2,2':6',2"-terpyridine (tpy), cisplatin, ethidium bromide (EB) and acridine orange (AO) were obtained from Alfa Aesar. MTT and PBS were obtained from Sigma-Aldrich. All other reagents and solvents were of high purity and used as received. Stock solutions of cisplatin (3 mM) were prepared in saline and **Ru1-Ru3** (10 mM) were prepared in DMSO. All stock solutions were stored at -20°C, thawed and diluted with culture medium prior to each experiment.

Microanalysis (C, H, and N) was carried out with a Vario EL elemental analyzer. ^{1}H-NMR spectra were recorded on a Varian INOVA Mercury-Plus 300 NMR spectrometer. Electrospray mass spectra (ES-MS) were recorded on a LCQ system (Finnigan MAT, USA). The spray voltage, tube lens offset, capillary voltage and capillary temperature were set at 4.50 KV, 30.00 V, 23.00 V and 200 ^{o}C, respectively, and the quoted *m/z* values are for the major peaks in the isotope distribution. UV-Vis spectra were recorded on a Perkin-Elmer Lambda 850 spectrophotometer. Emission spectra were recorded on a Perkin-Elmer LS 55 spectrofluorophotometer at room temperature

Synthesis

The terpyridyl ligands phtpy and biphtpy were synthesized according to the published literature[29] by changing appropriate substituted benzaldehyde.

Synthesis of Ru(N^N^N)Cl$_3$ To 125 mL of ethanol in a 200 mL round-bottom flask was added 262 mg (1 mmol) of $RuCl_3{\cdot}3H_2O$ and tpy (233 mg, 1mmol) phtpy (309 mg, 1mmol), biphtpy(385 mg, 1mmol), respectively . The mixture was heated at reflux for 8 h with vigorous magnetic stirring. After cooled to room temperature, and the fine brown powder which had appeared was filtered from the reddish yellow solution. The product was washed with 3 × 30 mL of ethanol followed by 3 × 30 mL of diethyl ether and air-dried. Yield: $Ru(tpy)Cl_3$ 61 %, $Ru(phtpy)Cl_3$ 56%, $Ru(biphtpy)Cl_3$ 45 %, respectively. The crude products were used without further purification.

Synthesis of [Ru(tpy)(bpy)Cl]ClO$_4$ (Ru1) A mixture of $Ru(tpy)Cl_3$ (0.044 g, 0.10 mmol), bpy (0.015 g, 0.1 mmol), triethylamine (1.0 mL), ethanol (9.0 mL) and distilled water (1.0 mL) was refluxed under argon for 10 h. After most of the ethanol was removed by rotary evaporation, a brownish-red precipitate was obtained by drop-wise addition of excess $NaClO_4$ solution. The product was purified by column chromatography on alumina using acetonitrile-toluene (2:1, v/v) as eluent. Yield: 60.2%. ES-MS (CH_3OH): *m/z* = 526.3 $[M - ClO_4]^+$. Anal. calcd. for $C_{25}H_{19}Cl_2N_5O_4Ru$: C, 48.01; H, 3.06; N, 11.20. Found: C, 47.89; H, 3.17; N, 11.04. ^{1}H NMR (300 MHz, d_6-DMSO): δ = 10.07 (d, *J* = 5.7 Hz, 1H), 8.88 (d, *J* = 6.0 Hz, 1H), 8.78 (d, *J* = 8.1 Hz, 2H), 8.66 (d, *J* = 8.1 Hz, 2H), 8.60 (d, *J* = 8.1 Hz, 1H), 8.33 (t, *J* = 7.8 Hz, 1H), 8.19 (t, *J* = 7.8 Hz, 1H), 8.04 (t, *J* = 7.8 Hz, 1H), 7.96 (t, *J* = 7.8 Hz, 2H), 7.75 (t, *J* = 7.8 Hz, 1H), 7.60 (d, *J* = 5.4 Hz, 2H), 7.35 (t, *J* = 6.9 Hz, 2H), 7.30 (d, *J* = 5.4 Hz, 1H), 7.05 (t, *J* = 7.2 Hz, 1H).

Synthesis of [Ru(phtpy)(bpy)Cl]ClO$_4$ (Ru2) A mixture of $Ru(phtpy)Cl_3$ (0.052 g, 0.10 mmol), bpy (0.015 g, 0.1 mmol), triethylamine (1.0 mL), ethanol (9.0 mL) and distilled water (1.0 mL) was refluxed under argon for 12 h. After most of the ethanol was removed by rotary evaporation, a brownish-red precipitate was obtained by drop-wise addition of excess $NaClO_4$ solution. The product was purified by column chromatography on alumina using acetonitrile-toluene (1:1, v/v) as eluent. Yield: 54.6%. ES-MS (CH_3OH): m/z = 602.0 $([M - ClO_4]^+)$. Anal. Calcd for $C_{31}H_{23}Cl_2N_5O_4Ru$: C, 53.07; H, 3.30; N, 9.98%. Found: C, 52.96; H, 3.45; N, 9.72%. ^{1}H NMR (300 MHz, d_6-DMSO) δ 10.08 (d, *J* = 5.4 Hz, 1H), 9.16 (s, 2H), 8.92 (d, *J* = 8.2 Hz, 3H), 8.63 (d, *J* = 7.7 Hz, 1H), 8.34 (t, *J* = 6.9 Hz, 1H), 8.30 (d, *J* = 8.1 Hz, 2H), 8.06 (t, *J* = 7.5 Hz, 1H), 8.00 (t, *J* = 7.5 Hz, 2H), 7.77 (t, *J* = 5.7 Hz, 1H), 7.69 (d, *J* = 7.2 Hz, 2H), 7.61 (m, 3H), 7.38 (dd, *J* = 12.6, 6.3 Hz, 3H), 7.06 (t, *J* = 6.0 Hz, 1H).

Synthesis of [Ru(biphtpy)(bpy)Cl]ClO$_4$ (Ru3) A mixture of $Ru(phphtpy)Cl_3$ (0.059 g, 0.10 mmol), bpy (0.015 g, 0.1 mmol), triethylamine (1.0 mL), ethanol (9.0 mL) and distilled water (1.0 mL) was refluxed under argon for 24 h. After most of the ethanol was removed by rotary evaporation, a brownish-red precipitate was obtained by drop-wise addition of excess $NaClO_4$ solution. The product was purified by column chromatography on alumina using acetonitrile-toluene (1:1, v/v) as eluent. Yield: 49.5%. ES-MS (CH_3OH): m/z = 678.1 $([M - ClO_4]^+)$. Anal. Calcd for $C_{37}H_{27}Cl_2N_5O_4Ru$: C, 57.15; H, 3.50; N, 9.01%. Found: C, 57.29; H, 3.66; N, 8.86%. ^{1}H NMR (300 MHz, d_6-DMSO) δ 10.09 (d, *J* = 4.6 Hz, 1H), 9.23 (s, 2H), 8.89 – 8.97 (m, 3H), 8.63 (d, *J* = 8.7 Hz, 1H), 8.43 (d, *J* = 6.9 Hz, 2H), 8.35 (t, *J* = 9.1 Hz, 1H), 8.05 – 7.99 (m, 5H), 7.86 (d, *J* = 8.1 Hz, 2H), 7.78 (d, *J* = 7.2 Hz, 1H), 7.62 (d, *J* = 4.2 Hz, 2H), 7.54 (t, *J* = 7.6 Hz, 2H), 7.46 – 7.35 (m, 4H), 7.08 (d, *J* = 3.3 Hz, 1H).

Aquation assay

Aquation of Ru(II) complex was monitored by UV-vis spectroscopy.[30] **Ru1-Ru3** were dissolved in DMSO and diluted with PBS buffer to give 30 μM solutions. The absorbance was recorded at 30 min intervals over 8 h at s310 K. Plots of the change in absorbance with time were fitted to the appropriate equation for pseudo first-order kinetics using Origin version 7.5 (Microcal Software Ltd.) to determine half-lives and rate constants.

Gel electrophoresis assay

Gel electrophoresis experiments[31]: DL5000 DNA marker was treated with different concentrations of **Ru1-Ru3** in 10 mM phosphate buffer (pH = 7.5), and the solution was kept at 37 °C for 1 h. Then, 2 μL of a quench buffer solution was added. The samples were analyzed by electrophoresis for 1.5 h at 80 V on a 0.8% agarose gel.

Log P$_{o/w}$ measurements

Log $P_{o/w}$ is the partition coefficient between octanol and water determined by the flask-shaking method.[32] An aliquot of a stock

View Article Online
DOI: 10.1039/C5DT02446C

solution of **Ru1-Ru3** in 100 mM aqueous NaCl (0.9% w/v to restrain aqueous and saturated with octanol) was added to an equal volume of octanol (saturated with 0.9% NaCl w/v) respectively. The mixture was shaken overnight at 60 rpm at 298 K to allow partitioning. After the sample was centrifuged at 3000 rpm for 10 min, the aqueous layer was carefully separated from the octanol layer for ruthenium analysis. The Ru concentration in the aqueous phase was determined by ICP-MS and used to calculate the $[Ru]_o/[Ru]_w$ ratio.

Cell culture and cytotoxicity test

The human cervix carcinoma cell line HeLa, the hepatocellular carcinoma cell lines Hep-G2 and BEL-7402, the lung carcinoma cell lines A549 and A549/CDDP, and the human normal hepatocyte cell line LO-2 were obtained from the Experimental Animal Center of Sun Yat-Sen University (Guangzhou, China). Cells were routinely maintained in DMEM (high glucose, HyClone) supplemented with 10% FBS (fetal bovine serum, HyClone), 50 U/mL streptomycin, and 50 ng/mL penicillin at 37 °C under a humidified atmosphere with 5% CO_2/95% air.

For cell cytotoxicity assay, approximately 1×10^4 cells/well were seeded in 96-well plates, followed by incubation in 5% CO_2 at 37°C for 24 h. After addition of serially diluted solutions of **Ru1-Ru3**, cells were than incubated for another 48 h. Finally, cytotoxicity was evaluated by the MTT assay; 20 μL of MTT solution (5 mg/mL in 1× PBS) was added to each well, followed by incubation for 4 h. The optical density of each well was then measured on a microplate spectrophotometer (Biorad, USA) at a wavelength of 595 nm..

ICP-MS assay

HeLa cells were plated at a density of 5×10^6 cells per100 mm Petri dish in 10 mL of culture medium.[33] On the second day, the cells were exposed to 10 μM **Ru1-Ru3**. After 6 h of drug exposure, the drug-containing medium was removed. The cells were washed twice with PBS and trypsinized, counted and divided into three portions. Half of the cells were centrifuged and washed with PBS for cytoplasm and nucleus fractionation analysis by a nucleus extraction kit (Pierce, Thermo) following the manufacturer's protocol. In the second portion, the cytoplasm was extracted using a cytoplasm extraction kit (Pierce, Thermo). The third half of the cells were used for Genomic DNA extraction for detection on ruthenium-DNA adducts using the Nucleon genomic DNA extraction kit (GE healthcare, Amersham, U.K.). The samples were digested with 60% HNO_3 at RT for one day. Each sample was diluted with MilliQ H_2O to obtain 2% HNO_3 sample solutions. The ruthenium concentration in each part was determined by inductively coupled plasma mass spectrometry inductively coupled plasma mass spectrometry (Thermo Elemental, USA).

EdU assay

EdU labeling was performed by using the Click-it EdU Alexa Fluor 594 imaging kit (Molecular Probes).[33] After incubating HeLa cells with 5 μM cisplatin and **Ru1-Ru3** for 24 h, 10 μM EdU (Molecular Probes) was added to the culture media and incubated for another 24 h. HeLa cells in 96-well plates were washed with 1× PBS, and 200 μL medium containing 10 μM EdU was then added to each well. The cells were incubated overnight and then washed with 1× PBS, followed by cell fixation with 4% polyphosphoric acid. After 15 min of incubation, the cells were washed twice with 3% BSA, followed by cell permeabilization using 0.5% Triton X-100 in 1× PBS and incubation for 20 min. The cells were then washed twice with 3% BSA, and 200 μL Click-iT reaction mixture was added, followed by 30 min incubation and one wash with 3% BSA. For nucleus staining, 200 μL of Hoechst 33342 solution was added to each well, and cells were incubated for another 30 min and washed twice with 200 μL of 1× PBS. The cells were finally imaged under an inverted fluorescence microscope (Zeiss Axio Observer Z1, Germany).

Acridine orange/ethidium bromide (AO/EB) staining

Cell apoptosis studies were performed with a staining method using acridine orange (AO) and ethidium bromide (EB).[34] HeLa cells was incubated in the absence or presence of **Ru1-Ru3** at a concentration of 5 μM at 37 °C and 5% CO_2 for 24 h. After 24 h, cells were stained with AO/EB solution (100 μg/mL AO, 100 μg/mL EB). Samples were observed under an inverted fluorescence microscope (Zeiss Axio Observer D1).

Generation and analysis of MCTSs

MCTSs were cultured using the liquid overlay method as reported by our lab previously.[33] HeLa cells in the exponential growth phase were dissociated by a trypsin/EDTA solution to gain single-cell suspensions. A number of 2500 diluted HeLa cells were transferred to 1% agarose-coated transparent 96-well plates with 200 μL of DMEM containing 10% serum. The cells would generate singlet MCTSs approximately 400 μm in diameter at day 4 with 5% CO_2 in air at 37 °C.

Cytotoxicity on 3D MCTSs

MCTSs of diameters approximate to 400 μm were treated with ruthenium(II) complexes and cisplatin by carefully replacing 50% of the medium with drug-supplemented standard medium using an 8-channel pipettor.[35] In parallel, for the untreated MCTSs, we replaced 50% of medium of the solvent-containing or solvent-free medium. Four MCTSs were treated per condition and drug concentration and the DMSO volume was less than 0.5% (v/v). The MCTSs were then allowed to incubate for another 72 h. The cytotoxicity of ruthenium complexes was measured by ATP concentration with a CellTiter-Glo Luminescent Cell Viability kit (Promega). After 20 minutes of incubation, the MCTSs were carefully transferred into black-sided, flat-bottomed 96-well plates (Corning) and pipette mixed for luminescence measurement on infinite M200 PRO equipment (TECAN)

Live/dead viability/cytotoxicity assay

The live/dead assay of MCTSs was performed using the LIVE/DEAD Viability/ Cytotoxicity Kit for mammalian cells (Life Technologies).[36] Live cells were distinguished by the presence of ubiquitous intracellular esterase activity, as determined by the enzymatic conversion of the virtually non-fluorescent cell-permeant calcein AM to the intensely fluorescent calcein (λ_{ex} = 495 nm, λ_{em} = 515 nm). EthD-1 would enter cells with damaged membranes and undergo a 40-fold enhancement of fluorescence upon binding to nucleic acids, thereby producing a

View Article Online
DOI: 10.1039/C5DT02446C

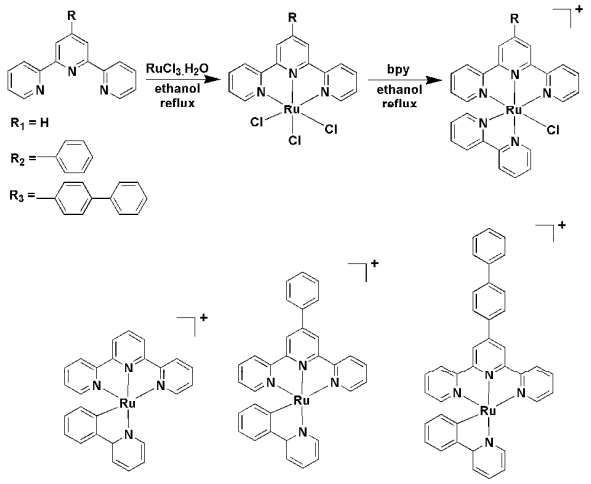

Scheme 1. Synthesis route and structures of **Ru1–Ru3**.

bright red fluorescence in dead cells (λ_{ex} = 495 nm, λ_{em} = 635 nm). Thus it was possible to determine cell viability depends on these physical and biochemical cell properties. After treatment with Ru(II) complexes, MCTSs were incubated with calcein AM (2 μM) and EthD-1 (4 μM) solutions for 30 min and imaged directly using an inverted fluorescence microscope (Zeiss Axio Observer D1, Germany).

Results and discussion

Synthesis and characterization

Ru1-Ru3 were synthesized by reacting the corresponding precursor with one equivalent amount of 2,2'-bipyridine in refluxing ethanol. All complex were purified by alumina column chromatography and characterized by ES-MS, elemental analysis and ^{1}H NMR spectroscopy (Fig. S1-S6).

Aquation of Chloride Ligand

Aquation of Ru-Cl bond was the an activated step for labile transition metal anticancer complex such as cisplatin which provides the possibility for metal center to coordinate with cellular macrobiological molecule such as DNA or protein. First of all, the aquation process of **Ru-Ru3** was tracked by UV-Vis spectroscopy. As shown in Fig. 1A and Fig.S7-S8, **Ru1-Ru3** gradually aquated in PBS buffer solution (PH=7.4). With incubation time extended, there was an apparent hypochromicity in the metal-to-ligand charge transfer (MLCT) band (440-600 nm), accompanied with a new absorbance band appeared (370-440 nm). The time-dependent absorptions of **Ru1-Ru3** at the indicated wavelengths follow pseudo-first-order kinetics (insets figure). The aquation rates of the complex follow the order: **Ru1** > **Ru2** > **Ru3** with a relative long half-life time (**Ru1**, $t_{1/2}$ = 1.5 h, **Ru2**, $t_{1/2}$ = 2.4 h, **Ru3**, $t_{1/2}$ = 3.0 h). Moreover, the *m/z* peak of $[Ru\text{-}Cl+H_2O]^+$ (Fig. 1B and Fig.S7-S8) also support the equated Ru(II) complex after incubation.

It has been well illustrated that chloride concentration have a significantly effect on the aquation of Cl-containing metal-based complex. The aquation degree of chloride ligand in present of different NaCl concentration was detected by ^{1}H NMR (Fig. 2).

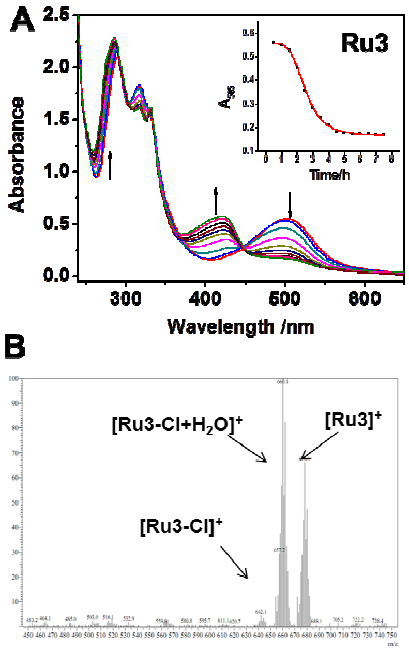

Fig. 1 (A) Aquation of **Ru3** in PBS buffer solution (pH = 7.4) tracking by UV-vis spectra. (B) LC-MS spectra of the aquated **Ru3**.

In the absent of NaCl, new peak in ^{1}H NMR spectra appeared with the incubation time extended and reached equilibrium. As expected, aquation of **Ru1-Ru3** were totally suppressed in present of 100 mM NaCl solution, a concentration similar to blood plasma (Fig. 2 and Fig. S9-S11). The aquation of **Ru1 - Ru3** in present of 4 mM NaCl (a concentration was similar to nucleus) was more readily than in 22 mM NaCl (a concentration was similar to cytoplasm). The dependence of aquation on chloride concentration may allow them to be selectively activated inside cancer cells with reduced side effects during transportation to cancer cells. Finally, the pK_a values of coordinated water were also determinded. The pK_a values have a significant influence on its reactivity since Ru-OH bond are often much less labile than Ru-OH_2 bond. The pK_a values of coordinated water were determined to be 7.32 ± 0.02 (**Ru1**), 7.50 ± 0.03 (**Ru2**) and 7.65 ± 0.03 (**Ru3**). Thus, **Ru1-Ru3** were thermodynamically stable and yet kinetically labile in buffer solution.

DNA binding studies

First of all, we determined whether **Ru1-Ru3** would exhibit stacking interaction in buffer solution at concentration between 1 to 100 μM. It was evident in Fig. S12-14 that no significant stacking interaction was observed for **Ru1-Ru3**.

Gel electrophoresis could provide an intuitive view to determine whether compounds exhibit DNA binding activity.[37] Cisplatin bind DNA covalentlyy which result in reduced DNA gel electrophoretic mobility.[38] The interaction of plasmid DNA with **Ru1-Ru3** were investigated (Fig. S15). **Ru3** was found to impede the migration of pUC19 DNA with increasing complex concentration. In contrast, **Ru1** and **Ru2** were less efficient though both of them also formed covalently binding with DNA. These results implied that **Ru3** can bind DNA by intercalation besides covalent binding.

View Article Online
DOI: 10.1039/C5DT02446C

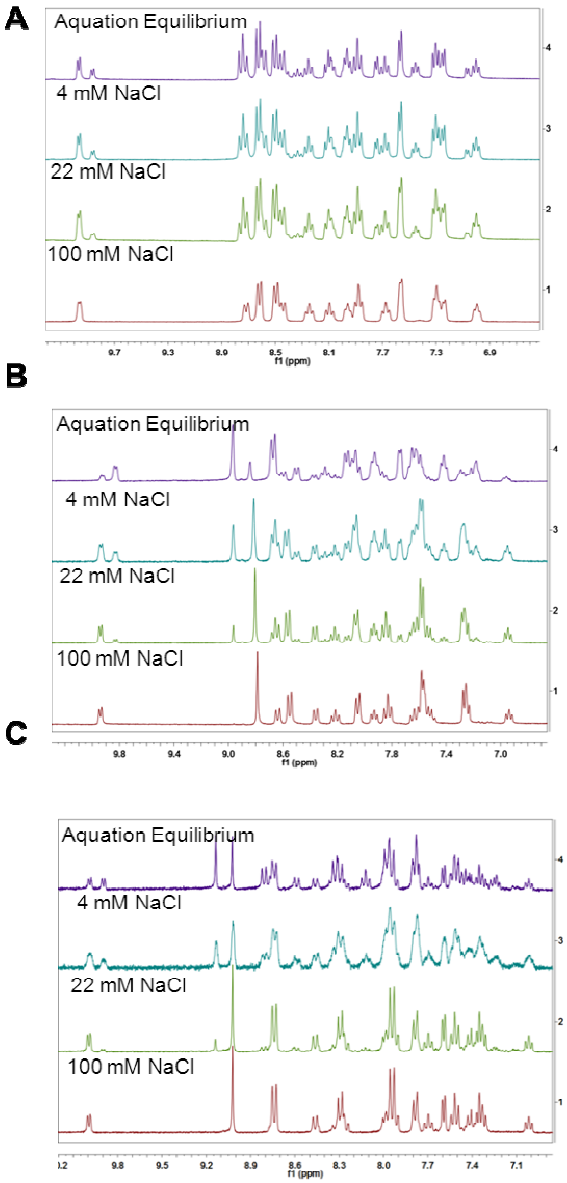

Fig. 2 Aquation of **Ru1-Ru3** (A, B and C, respectively) in present of different concentration of NaCl detected by ^{1}H NMR.

In recent years, MALDI-TOF MS (martix-assisted laser desorption ionization-time of flight mass spectrum) has been used to determinded the formation of metal-DNA adducts.[39] The covalent binding of **Ru1-Ru3** in present of double-stranded oligonucleotides OD1 and OD2 were investigated. As shown in Fig. S16 free oligonucleotides OD1 ($[M-H]^-$) and OD2 ($[M-H]^-$) could be clearly oberved. The spectra of **Ru3**-bound oligonucleotides increased gradually whereas the peak of OD1 and OD2 decreased as incubation time extended. No peak at m/z values over 6000 could be observed, suggesting that none of the Ru(II) complexes formed interstrand cross-linking adducts. The reduced peak intensity of oligonucleotides after adding Ru(II) complexes confirmed covalently binding activity of **Ru1-Ru3** with DNA.

Hydrophobicity Measurements

Log $P_{o/w}$ value is the partition coefficient between octanol and water. By extending the phenyl-terpyridyl ligand, the log $P_{o/w}$ value increased gradually. **Ru3** (0.63) tend to be more hydrophobic than **Ru1** (-1.1) and **Ru2** (-0.35). The positive log $P_{o/w}$ value of **Ru3** may facilitate its cell uptake efficiency and enhance anticancer activities.

Table 1 IC_{50} (μM) values of **Ru1-Ru3**.

Complexes	LO2	Hep-G2	BEL-7402	A549	A549R	HeLa	HeLa MCTSs
Ru1	>100	>100	>100	>100	>100	>100	>100
Ru2	>100	69.2	45.3	79.2	>100	51.4	>100
Ru3	10.2	5.6	7.4	3.7	4.1	3.3	8.5
Cisplatin	9.6	11.8	12.4	6.4	45.2	10.5	50.7

Cytotoxicity assay

MTT assay was used to evaluate the anticancer activity of **Ru1-Ru3**. Five human tumor cell lines, HeLa, Hep-G2, BEL-7402 A549, A549R and a normal cell line LO-2, were determined (Table 1). **Ru1** was nontoxic toward all cancer cells tested as well as normal cells (IC_{50} >100 μM). The introduction of phenyl in tpy ligand resulted in slightly increase in anticancer activity with IC_{50} values ranging from 40 - 80 μM. Surprisingly, with regard to biphenyl-substituted **Ru3**, significant enhanced anticancer activity was observed. The IC_{50} values of **Ru3** toward cancer cells were even lower than that of cisplatin. **Ru3** was also active against cisplatin-resistant A549R cells with IC_{50} value similar to the A549 cells. Additionally, all Ru(II) complex exhibited lower cytotoxicity toward the normal cell line than cisplatin.

Cell Uptake Analysis

The high sensitivity of ICP-MS (inductively coupled plasma mass spectrometry) makes it a practical method to detect and identify metal-based complex within cells. The accumulation of **Ru1-Ru3** into nucleus and cytoplasm were studied. The total ruthenium concentration within cells was in excellent agreement with log $P_{o/w}$ data in the order **Ru3** > **Ru2** > **Ru1**. For all complexes, the highest concentration of ruthenium was found in the cytoplasm (Fig. 3). As the length of terpyridyl ligand extended, the amount of ruthenium accumulated in nucleus increased significantly. Since **Ru1-Ru3** underwent aquation and bound DNA covalently, genome DNA of HeLa cells after drug treatment was isolated to determine the levels of DNA-bound ruthenium within cells. Although the concentration of DNA-bound ruthenium was not very high even for **Ru3**, the correlation

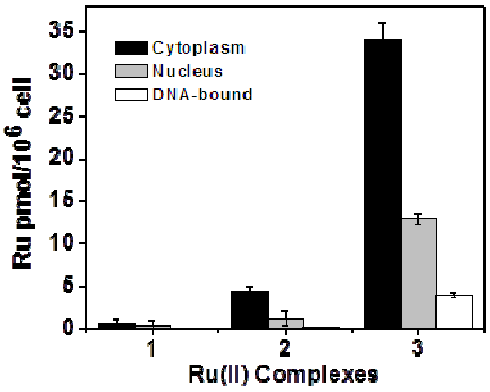

Fig. 3 Cellular ruthenium distribuction within HeLa cells..

View Article Online
DOI: 10.1039/C5DT02446C

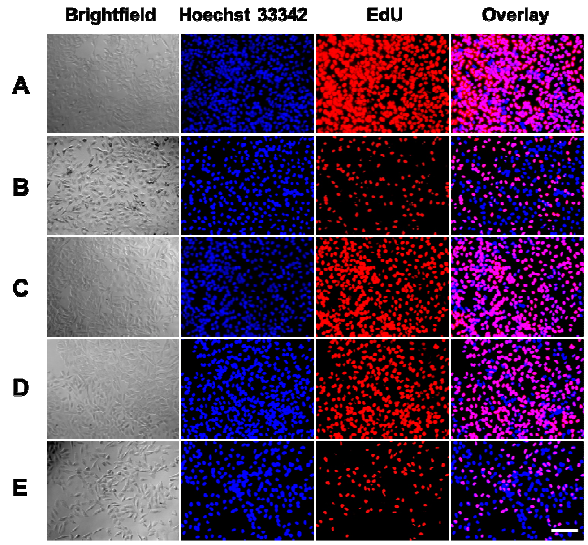

Fig. 4 EdU antiproliferation assay. (A) cells without treatment, (B) cells treated with 10 μM cisplatin, (C−E) cells treated with **Ru1-Ru3** (5 μM). Blue fluorescence represented Hochest 33342. Red fluorescence represented EdU. Scale bars = 100 μm.

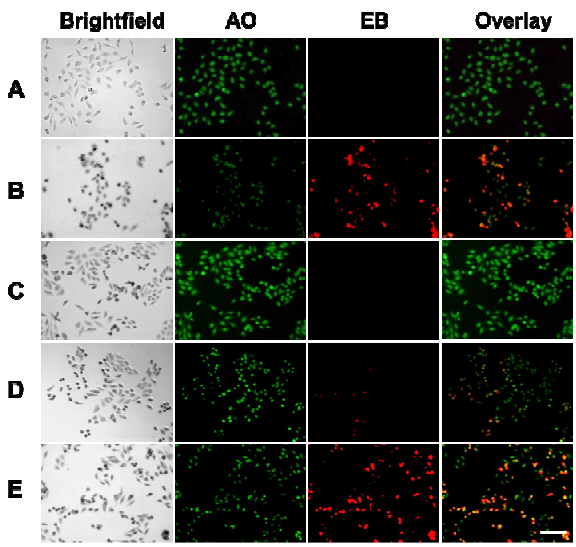

Fig. 5 HeLa cells were stained by AO/EB and observed under a fluorescence microscope after 48 h drug exposures. (A) cells without treatment, (B) cells treated with 10 μM cisplatin, (C−E) HeLa cells treated with **Ru1-Ru3** (5 μM). Scale bars = 100 μm.

between nucleus accumulation and cell cytotoxicity was apparent. **Ru3** with the most extended terpyridyl ligand exhibited the highest level of ruthenium within nucleus and most cytotoxic.

Antiproliferative Effect on HeLa Cells

EdU (5-ethynyl-2′-deoxyuridine) was a thymidine analog that can incorporat into DNA replication, serving as a fluorescence marker of active proliferating cells.[41-43] EdU detection relies on a simple and quick click reaction that does not necessitate a DNA denaturation step like BdrU detection. For cells without drug treatment, a large number of newly replicated DNA were detected in the cell nuclei (Fig. 4), while DNA replication process was dramatically reduced after incubating with cisplatin. For Ru(II) complex, only **Ru3** could distinctly inhibit DNA synthesis process, while **Ru1** and **Ru2** were less effective. This result was in agreement with cell uptake assay since only **Ru3** can penetrate into cell nucleus.

Then, we identified the cellular response after treatment with the Ru(II) complex using the acridine orange/ethidium bromide (AO/EB) dual staining assay (Fig. 5). AO is a vital dye and can stain both live and dead cells. EB stains only cells that have lost their membrane integrity. Under the fluorescence microscope, live cells appear green. Necrotic cells stain orange red but have a nuclear morphology resembling that of viable cells. Apoptotic cells appear green, and morphological changes such as cell blebbing and formation of apoptotic bodies will be observed. After a 48 h treatment, **Ru1** and **Ru2** (5.0 μM) did not induce apparent cell apoptosis because the cells were only stained by AO (green). A large amount of apoptosis cells appeared after incubation with **Ru3** (5.0 μM) or cisplatin (10.0 μM).

Generation and analysis of MCTSs

In recent years, 3D multicellular tumor spheroids (MCTSs) functioned as a better choice for *in vitro* negative anticancer drug selection rather traditional cancer cell monolayer. MCTSs restores the *in vivo*-like extracellular matrix (ECM) and is capable of mimicking therapeutic problems associated with metabolic and proliferative gradients found in solid tumors, such as the altered responsiveness of chronically hypoxic tumor cells, and multidrug resistance to chemotherapy drugs.[44-45] Several methods have been designed to generate tumor spheroids, among which the agarose-coated liquid-overlay 96-well plate culture provided an easy-handling and high throughput protocol for generating single MCTSs in each 96 well.[46-48] This method exhibited desirable characteristics: (i) 96-well suspension culture; (ii) a single spheroid per well; (iii) high reproducibility; and (iii) simple harvesting for further analysis.

Cytotoxicity on 3D MCTSs cancer model

Cancer cells within solid tumor are generally less sensitive to chemotherapeutics than cultured cancer cell monolayer. MCTSs with diameters of approximately 400 μm have been suggested to be a better choice than small MCTSs because they can better resemble the pathophysiological conditions of solid tumors, such as the specific hypoxic areas in the center and proliferation gradients than small spheroids.[49] We thus tested the cytotoxicity of **Ru-Ru3** and cisplatin on MCTSs with diameter around 400 μm. The IC_{50} values of cisplatin (50 μM) were almost 5 times higher than treating with cancer cell monolayer (10.5 μM), indicated significant multicellular drug resistance. Under the same conditions, the IC_{50} values of **Ru3** was 8.5 μM, nearly 3 times higher than the concentrations used with the cancer cell monolayer. In contrast, **Ru1** and **Ru2** were totally inactive against MCTSs (above 100 μM). These data indicated that **Ru3** exhibited superior anticancer activity than cisplatin no matter on 2D cancer cell monolayer or 3D MCTSs.

The survival condition of MCTSs following drug treatment was investigated by live/dead viability/cytotoxicity assay after exposure to drugs. The virtually non-fluorescent cell-permeant calcein AM will change to a green fluorescent species by intracellular esterases in living cells. In contrast, EthD-1 could simply enter dead cells and emit red fluorescence upon binding to nucleic acids.[50] As shown in Fig. 6, untreated MCTSs as well

View Article Online
DOI: 10.1039/C5DT02446C

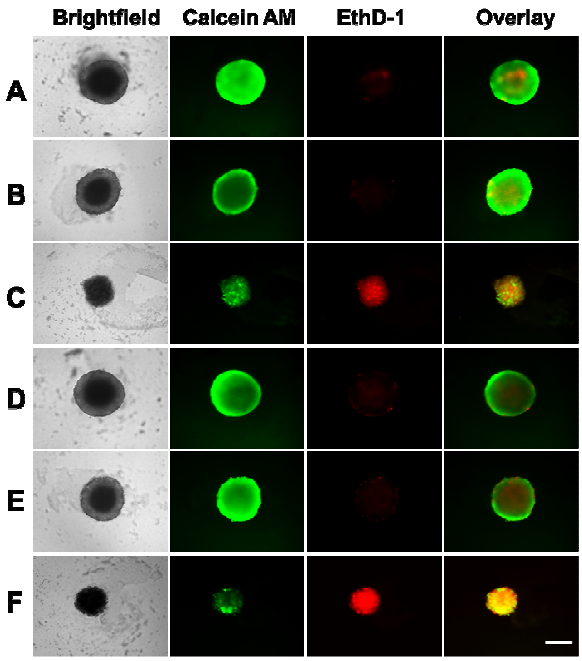

Fig. 6 Calcein AM and EthD-1 dual-staining on drug-treated HeLa MCTSs. (A) MTCSs without treatment, (B) MTCSs treated with 10 μM cisplatin, (C) MTCSs treated with 50 μM cisplatin, (D−F) MTCSs treated with **Ru1-Ru3** (10 μM), respectively. Scale bars = 200 μm.

as MCTSs treated with 10 μM cisplatin emitted steady green fluorescence from the whole spheroid, suggesting no cell death occurred within MCTSs. The dead cells appeared after treated with 50 μM cisplatin. The green fluorescence significantly weakened and bright red fluorescence appeared when the MCTSs were treated with 10 μM of **Ru3**. Besides, the volume of MCTSs reduced significantly compared with untreated MCTSs, indicating severe cell damage had occurred. In contrast, complexes **Ru1** and **Ru2** (100 μM) did not show any impressive cytotoxic effect on the MCTSs.

Structure-activity relationship

Compared with organic small molecules, metal complexes offer several distinct advantages as therapeutic agents or biomolecular probes.[51-53] Our group have previously reported coordinatively saturated polypyridyl Ru(II) complexes for anticancer drug screening. Although these Ru(II) complexes exhibited excellent *in vitro* DNA transcription inhibition or topoisomerase inhibitory activity, most of which presented impressive cytotoxicity when evaluated against cancer cells (IC_{50} between 50-490 μM).[54-58] Such unexpected results impeled us to explore the intrinsic structure-anticancer activity relationship of polypyridyl Ru(II) complexes with the hope to increase anticancer activity. Barton et al systematically explored the cellular uptake and localization of a series of Ru(II) complexes containing intercalative ligand, and found that the complex with the greatest lipophilicity exhibited the greatest uptake.[32] However, while changes in hydrophobicity can modulate cellular uptake, this chemical property can also lead to cytoplasm localization of the complex and reduced nuclear targeting. In the present study, the above results indicate that extending the tpy ligand with phenyl-substituent may be an effective method to improve hydrophobicity of Ru(II) complexes and thus enhance cell uptake efficiency and anticancer activity.

Conclusions

In conclusion, this study presented a valid procedure to increase anticancer activity of terpyridyl Ru(II) complex. **Ru1-Ru3** shared different length of phenyl-substituted tpy ligand exhibited a huge different in anticancer activity. **Ru3** with biphenyl-tpy ligand exhibit the higher DNA binding affinity and anticancer activity than **Ru1** and **Ru2**. The positive log $P_{o/w}$ value, high cell uptake efficiency and nucleus distribution of **Ru3** may contribute to its excellent anticancer activity on cell monolayer and 3D MCTSs. Cell proliferation assay and cell apoptosis experiments revealed that **Ru3** mainly induced cancer cells apoptosis. Taken together, our research opened new approach for the design of terpyridyl Ru(II) anticancer complex.

Acknowledgments

This work was supported by the 973 program (No. 2015CB856301), the National Science Foundation of China (Nos. 21172273, 21171177, 21471164, and J1103305), the Program for Changjiang Scholars and Innovative Research Team in the University of China (No. IRT1298), and the National High Technology Research and Development Program of China (863 Program, 2012AA020305).

Notes and references

MOE Key Laboratory of Bioinorganic and Synthetic Chemistry, School of Chemistry and Chemical Engineering, Sun Yat–Sen University, Guangzhou, 510275, P. R. China. Email: cesjln@mail.sysu.edu.cn, ceschh@mail.sysu.edu.cn

† Electronic Supplementary Information (ESI) available: Figures of ES-MS, ^{1}H-NMR, DNA gel electrophoretic mobility. See DOI:10.1039/b000000x

1 L. H. Hurley, *Nat. Rev. Cancer*, 2002, **2**, 188-200.
2 R. Palchadhuri and P. J. Hergenrother, *Curr. Opin. Biotechnol.*, 2007, **18**, 497-503.
3 A. J. Pickard and U. Bierbach, *ChemMedChem*, 2013, **8**, 1441-1449.
4 B. L. Bloodgood, N. Sharma, H. A. Browne, A. Z. Trepman, M. E. Greenberg, *Nature*, 2013, **503**, 121-125.
5 X. Wang and J. Z. Guo, *Chem. Soc. Rev.*, 2013, **42**, 202-224.
6 C. A. Rabik and M. E. Dolan, *Cancer Treat. Rev.*, 2007, **33**, 9-23.
7 K. Irena, *Curr. Med. Chem.*, 2006, **13**, 1085-1107.
8 W. X. Ni, W. L. Man, S. M. Yiu, M. Ho, M. T. W. Cheung, C. C. Ko, C. M. Che, Y. W. Lam, T. C. Lau, *Chem. Sci.*, 2012, **3**, 1582-1588.
9 R. C. Todd and S. J. Lippard, *Metallomics*, 2009, **1**, 280-291.
10 A. C. Komor and J. K. Barton, *Chem. Commun.*, 2013, **49**, 3617-3630.
11 F. Kratz, M. Hartmann and B. Keppler, *J. Biol. Chem.*, 1994, **269**, 2581-2588.
12 G. N. Kaluderović and R. Paschke, *Curr. Med. Chem.*, 2011, **18**, 4738-4735.
13 M. Galanski, V. B. Arion, M. A. Jakupec and B. K. Keppler, *Curr. Pharm. Des.*, 2003, **9**, 2078-2789.
14 S. L. F. Chan, R. W. Y. Sun, M. Y. Choi, Y. Zeng, L. Shek, S. S. Y. Chui and Chi-Ming Che, *Chem. Sci.*, 2011, **2**, 1788-1792.
15 C. G. Hartinger, M. A. Jakupec, S. Zorbas-Seifried, M. Groessl, A. Egger, W. Berger, H. Zorbas, P. J. Dyson and B. K. Keppler, *Chem. Biodivers.*, 2008, **5**, 2140-2155;
16 V. Vidimar, X. Meng, M. Klajner, C. Licona, L. Fetzer, S. Harlepp, P. Hebraud, M. Sidhoum, C. Sirlin, J. P. Loeffler, G. Mellitzer, G.

View Article Online
DOI: 10.1039/C5DT02446C

Sava, M. Pfeffer and C. Gaiddon, *Biochem. Pharmacol.*, 2012, **84**, 1428-1436.
17 O. Tredan, C. M. Galmarini, K. Patel and I. F. Tannock, *J. Natl. Cancer Inst.*, 2007, **99**, 1441-1454.
18 A. Abbott, *Nature*, 2003, **424**, 870-872.
19 F. Pampaloni, E. G. Reynaud and E. H. Stelzer, *Nat. Rev. Mol. Cell. Biol.*, 2007, **8**, 839-845.
20 G. Mazzoleni, D. Di Lorenzo and N. Steimberg, *Genes Nutr.*, 2009, **4**, 13-22.
21 L. Hutchinson and R. Kirk, *Nat. Rev. Clin. Oncol.*, 2011, **8**, 189-190.
22 A. I. Minchinton and I. F. Tannock, *Nat. Rev. Cancer*, 2006, 6, 583-592.
23 J. L. Horning, S. K. Sahoo, S. Vijayaraghavalu, S. Dimitrijevic, J. K. Vasir, T. K. Jain, A. K. Panda and V. Labhasetwar, *Mol. Pharm.*, 2008, **5**, 849-862.
24 S. Ghosh, G. C. Spagnoli, I. Martin, S. Ploegert, P. Demougin, M. Heberer and A. Reschner, *J. Cell. Physiol.*, 2005, **204**, 522-531.
25 P. C. De Witt Hamer, A. A. Van Tilborg, P. P. Eijk, P. Sminia, D. Troost, C. J. Van Noorden, B. Ylstra and S. Leenstra, *Oncogene*, 2008, **27**, 2091-2096.
26 A. Sivaraman, J. K. Leach, S. Townsend, T. Iida, B. J. Hogan, D. B. Stolz, R. Fry, L. D. Samson, S. R. Tannenbaum and L. G. Griffith, *Curr. Drug Metab.*, 2005, **6**, 569-591.
27 J. Friedrich, R. Ebner and L. A. Kunz-Schughart, *Int. J. Radiat. Biol.*, 2007, **83**, 849-871.
28 C. Fischbach, R. Chen, T. Matsumoto, T. Schmelzle, J. S. Brugge, P. J. Polverini and D. J. Mooney, *Nat. Methods*, 2007, **4**, 855-860.
29 D. N. Chirdon, W. J. Transue, H. N. Kagalwala, A. Kaur, A. B. Maurer, T. Pintauer and S. Bernhard, *Inorg. Chem.*, 2014, **53**, 1487-1499.
30 S. H. van Rijt, A. Mukherjee, A. M. Pizarro and P. J. Sadler, *J. Med. Chem.*, 2010, **53**, 840-849.
31 H. Y. Huang, P. Y. Zhang, H. M. Chen, L. N. Ji and H. Chao, *Chem. Eur. J.*, 2015, **21**, 715-725.
32 C. A. Puckett and J. K. Barton, *J. Am. Chem. Soc.*, 2007, **129**, 46-47.
33 H. Y. Huang, P. Y. Zhang, B. L. Yu, Y. Chen, J. Q. Wang, L. N. Ji and H. Chao, *J. Med. Chem.*, 2014, **57**, 8971-8983.
34 P. Y. Zhang, J. Q. Wang, H. Y. Huang, L. P. Qiao, L. N. Ji and H. Chao, Dalton Trans., 2013, **42**, 8907-8917.
35 B. S. Howerton, D. K. Heidary and E. C. Glazer, *J. Am. Chem. Soc.*, 2012, **134**, 8324 –8327.
36 L. F. Yu, M. C. W. Chen and K. C. Cheung, *Lab Chip*, 2010, 10, 2424– 2432.
37 T. N. Singh and C. Turro, *Inorg. Chem.*, 2004, **43**, 7260-7262.
38 M. Bien, F. P. Pruchnik, A. Seniuk, T. M. Lachowicz and P. Jakimowicz, *J. Inorg. Biochem.*, 1999, **73**, 49-55.
39 S. Redon, S. Bombard, M. A. Elizondo-Riojas and J. C. Chottard, *Nucleic Acids Res.*, 2003, **31**, 1605-1613.
40 Z. Liu, A. Habtemariam, A. M. Pizarro, S. A. Fletcher, A. Kisova, V. Oldrich, L. Salassa, P. C. A. Bruijnincx, G. J. Clarkson, V. Brabec and P. J. Sadler, *J. Med. Chem.*, 2011, **54**, 3011-3026.
41 A. Salic and T. J. Mitchison, *Proc. Natl. Acad. Sci.*, 2008, **105**, 2415-2420
42 H. J. Yoon, T. H. Kim, Z. Zhang, E. Azizi, T. M. Pham, C. Paoletti, J. Lin, N. Ramnath, M. S. Wicha, D. F. Hayes, D. M. Simeone and S. Nagrath, Nat. Nanotechnol., 2013, 8, 735-741.
43 M. J. Levesque and A. Raj, *Nat Methods*, 2013, **10**, 246-248.
44 R. M. Sutherland, *Science*, 1988, **240**, 177-184.
45 K. E. LaRue, M. Khalil and J. P. Freyer, *Cancer Res.*, 2004, **64**, 1621–1631.
46 G. Y. Lee, P. A. Kenny, E. H. Lee and M. J. Bissell, *Nat. Methods*, 2007, **4**, 359-365.
47 Y. Matsuda, T. Ishiwata, Y. Kawamoto, K. Kawahara, W. X. Peng, T. Yamamoto and Z. Naito, *Med. Mol. Morphol.*, 2010, **43**, 211-217.
48 S. Takaishi, T. Okumura, S. Tu, S. S. Wang, W. Shibata, R. Vigneshwaran, S. A. Gordon, Y. Shimada and T. C. Wang, *Stem Cells*, 2009, **27**, 1006-1020.
49 M. Vinci, S. Gowan, F. Boxall, L. Patterson, M. Zimmermann, W. Court, C. Lomas, M. Mendiola, D. Hardisson and S. A. Eccles, *BMC Biol.*, 2012, **10**, 29.
50 T. Yogo, Y. Urano, Y. Ishitsuka, F. Maniwa and T. Nagano，*J. Am. Chem. Soc.*, 2005, 127, 12162-12163.
51 C. H. Leung, H. J. Zhong, H. Yang, Z. Cheng, D. S. Chan, V. P. Ma, R. Abagyan, C. Y. Wong and D. L. Ma, *Angew. Chem. Int. Ed.*, 2012 **51**, 9010-9014.
52 D. L. Ma, D. S. H. Chan and C. H. Leung, *Acc. Chem. Res.*, 2014, **47** 3614-3631.
53 C. H. Leung, H. J. Zhong, D. S. H. Chan and D. L. Ma, *Coord. Chem. Rev.*, 2013, **257**, 1764-1776.
54 K. J. Du, J. Q. Wang, J. F. Kou, G. Y. Li, L. L. Wang, H. Chao and L. N. Ji, *Eur. J. Med. Chem*., 2011, **46**, 1056-1065.
55 P. Y. Zhang, J. Q. Wang, H. Y. Huang, L. P. Qiao, L. N. Ji and H. Chao, *Dalton Trans.*, 2013, **42**, 8907-8917.
56 C. Qian, J. Q. Wang, C. L. Song, L. L. Wang, L. N. Ji and H. Chao, *Metallomics*, 2013, **5**, 844-854.
57 Y. C. Wang, C. Qian, Z. L. Peng, X. J. Hou,, L. L. Wang, H. Chao and L. N. Ji, *J. Inorg. Biochem*., 130 (2014) 15-27.
58 F. Gao, X. Chen, J. Q. Wang, Y. Chen, H. Chao and L. N. Ji, *Inorg. Chem.*, 2009, **48**, 5599-5601.